

Diagnosing postoperative lymph node metastasis in thyroid cancer with multimodal radiomics and clinical features

DIGITAL HEALTH
Volume 10: 1–11
© The Author(s) 2024
Article reuse guidelines:
sagepub.com/journals-permissions
DOI: 10.1177/20552076241233244
journals.sagepub.com/home/dhj



Xin Fan^{1,2}, Han Zhang^{1,2}, Zhengshi Wang^{3,4}, Xiaoying Zhang^{1,2},
Shanshan Qin^{1,2}, Jiajia Zhang^{1,2}, Fan Hu^{1,2}, Mengdie Yang^{1,2},
Jingjing Zhang^{5,6,7} and Fei Yu^{1,2} 

Abstract

Purpose: This study aims to evaluate the diagnostic value of texture analysis for lymph node metastasis after thyroid cancer surgery.

Methods: We retrospectively analyzed patients who underwent positron emission tomography/computed tomography (PET/CT) examination before ¹³¹I treatment at Shanghai Tenth People's Hospital between 2017 and 2020. Clinical follow-up results were used as the criterion for determining the presence of lymph node metastasis. The study included 119 patients, who were then randomly divided into training and test groups in a 7:3 ratio. Regions of interest were identified, and radiomics features were extracted using LIFEx 7.3.0. Mann–Whitney U test and LASSO regression were employed to screen radiomics parameters for modeling. Subsequently, a nomogram model was built by combining radscore and clinical features. SPSS 26.0 software was utilized for statistical analysis, and $p < 0.05$ was considered statistically significant.

Results: Follow-up confirmed 54 patients with thyroid cancer lymph node metastasis and 65 patients in the non-metastasis group. A total of 119 lymph nodes were delineated. For each lesion, 164 CT texture features and 164 PET texture features were extracted, and 107 significant parameters were identified, including 16 CT texture parameters and 91 PET texture parameters. After screening, 3 CT parameters, 4 PET parameters and 12 PET/CT parameters were selected to establish three radiomic models. The AUC values were as follows: AUC (CT) = 0.730, AUC (PET) = 0.759 and AUC (PET/CT) = 0.864. We then combined clinical features and radscore to construct a nomogram, resulting in a C-index of 0.915 in the training group. In the test group, the C-index was confirmed to be 0.868.

Conclusions: Radiomics may enhance the diagnostic efficiency of lymph node metastases after thyroid cancer surgery and could potentially assist clinicians in future diagnoses. The developed nomogram, which combines radiomics and clinical features, offers relatively high accuracy in helping clinicians assess the risk of metastasis in thyroid patients after surgery.

¹Department of Nuclear Medicine, Shanghai Tenth People's Hospital, Tongji University School of Medicine, Shanghai, China

²Institute of Nuclear Medicine, Tongji University School of Medicine, Shanghai, China

³Thyroid Center, Shanghai Tenth People's Hospital, Tongji University School of Medicine, Shanghai, China

⁴Shanghai Center of Thyroid Diseases, Shanghai Tenth People's Hospital, Tongji University School of Medicine, Shanghai, China

⁵Department of Diagnostic Radiology Yong Loo Lin School of Medicine, National University of Singapore, Singapore, Singapore

⁶Clinical Imaging Research Centre, Centre for Translational Medicine, Yong Loo Lin School of Medicine, National University of Singapore, Singapore, Singapore

⁷Nanomedicine Translational Research Program, NUS Center for Nanomedicine, Yong Loo Lin School of Medicine, National University of Singapore, Singapore, Singapore

Corresponding authors:

Jingjing Zhang, Department of Diagnostic Radiology Yong Loo Lin School of Medicine, National University of Singapore, Singapore, Singapore; Clinical Imaging Research Centre, Centre for Translational Medicine, Yong Loo Lin School of Medicine, National University of Singapore, Singapore, Singapore; Nanomedicine Translational Research Program, NUS Center for Nanomedicine, Yong Loo Lin School of Medicine, National University of Singapore, Singapore, Singapore.
Email: j.zhang@nus.edu.sg

Fei Yu, Department of Nuclear Medicine, Shanghai Tenth People's Hospital, Tongji University School of Medicine, Shanghai, China; Institute of Nuclear Medicine, Tongji University School of Medicine, Shanghai, China.
Email: yufei_021@163.com

Xin Fan, Han Zhang and Zhengshi Wang contributed equally to this work.



Keywords

Post-surgical managements, differentiated thyroid cancer, lymph node metastasis, clinical risk factors

Submission date: 8 July 2023; Acceptance date: 31 January 2024

Introduction

Thyroid cancer is the most prevalent malignant tumor in the head and neck and endocrine systems. Differentiated thyroid carcinoma (DTC), which includes papillary thyroid carcinoma (PTC) and follicular thyroid carcinoma (FTC), accounts for approximately 90% of all thyroid cancers, with PTC being the most common.¹ Although the mortality rate of DTC is low and the prognosis for most patients is favorable following standardized treatment, some patients still develop distant metastasis and progress to radioiodine refractory differentiated thyroid carcinoma (RAIR-DTC). Cervical lymph nodes are the most frequent sites of extrathyroidal metastasis in PTC, and lymph node metastasis is an independent risk factor for PTC recurrence.²

Radioactive iodine (RAI) therapy is a crucial treatment modality after thyroid cancer surgery, as it can reduce the risk of recurrence in high-risk thyroid cancer patients.³ Before RAI treatment, it is essential to evaluate the patient's condition to determine the appropriate dose and therapeutic response to different radioiodine activities.⁴ However, additional radionuclide treatment may cause unnecessary side effects and even increase the incidence of other tumors.^{5,6} Therefore, accurately evaluating a patient's condition before RAI and determining the presence of lymph node metastasis is critical.

Currently, ¹⁸F-FDG PET/CT imaging exhibits significant variation in diagnostic accuracy and lacks clear indicators for postoperative lymph node metastasis in thyroid cancer. Accurate determination of lymph node metastasis after thyroid surgery is crucial for treatment selection and prognosis. Radiomics features are quantitative image features that provide information on tumor intensity, shape, size, volume and texture. PET radiomics primarily analyze the texture and metabolic characteristics of lesions to reflect their molecular biological function, while CT radiomics focus on analyzing morphological features of lesions to represent their anatomical and pathological structures. PET/CT radiomics can more comprehensively reflect the internal function and structure of tumors, assisting clinicians in selecting appropriate treatment options and evaluating prognosis more effectively.

Recent guidelines and literature reviews show that PET/CT has become a valuable tool in the management of DTC patients, particularly in the initial evaluation of intermediate and high-risk DTC patients.^{7,8} However, there are

limited studies on PET/CT-based multimodal radiomics. Thyroglobulin (Tg) is a common clinical monitoring method after thyroid cancer surgery, as most patients have residual thyroid glands after the initial surgery.⁹ Residual glands secrete Tg, but Tg evaluation alone may produce misleading results, necessitating imaging evaluation.¹⁰ Some other studies have reported analysis of the risk and prognosis of lymph node metastasis in thyroid cancer based on clinical features, but the supplementary performance of imaging features is lacking and needs to be further improved.^{11–13} Current imaging methods for thyroid cancer lymph node metastasis have low diagnostic efficiency and exhibit significant variation. Therefore, we use PET/CT multi-modal imaging data and combine the advantages of radiomics to improve the diagnostic efficiency of lymph node metastasis. To our current knowledge, this is the first study to apply multimodal radiomics in the diagnosis of lymph node metastasis.

This study aims to predict the presence of residual lymph node lesions after thyroid cancer surgery, enhance the accuracy of diagnosis and treatment effectiveness and improve the prognosis for PTC patients.

Methods and materials

Study population

This retrospective study was approved by the Institutional Review Committee of Shanghai Tenth People's Hospital (SHYS-IEC-5.0/22K263/P01) and registered with the Chinese Clinical Trials Registry (ChiCTR2200065342). We collected clinical information and imaging data from thyroid cancer patients treated with radioactive iodine at Shanghai Tenth People's Hospital between December 2017 and July 2020. A total of 152 patients who underwent ¹⁸F-FDG PET/CT within one week before RAI following thyroid cancer surgery and had complete pathological information were included.

Exclusion criteria were as follows: short follow-up time after the first ¹³¹I treatment (less than 7 months), preventing accurate determination of lesion metastasis; inability to outline lymph node margins; previous antitumor therapy or radiotherapy before PET/CT; presence of other types of tumors and fewer than 64 voxels. Based on these exclusion criteria, 33 patients were excluded and the remaining 119 patients underwent texture analysis (Figure 1).

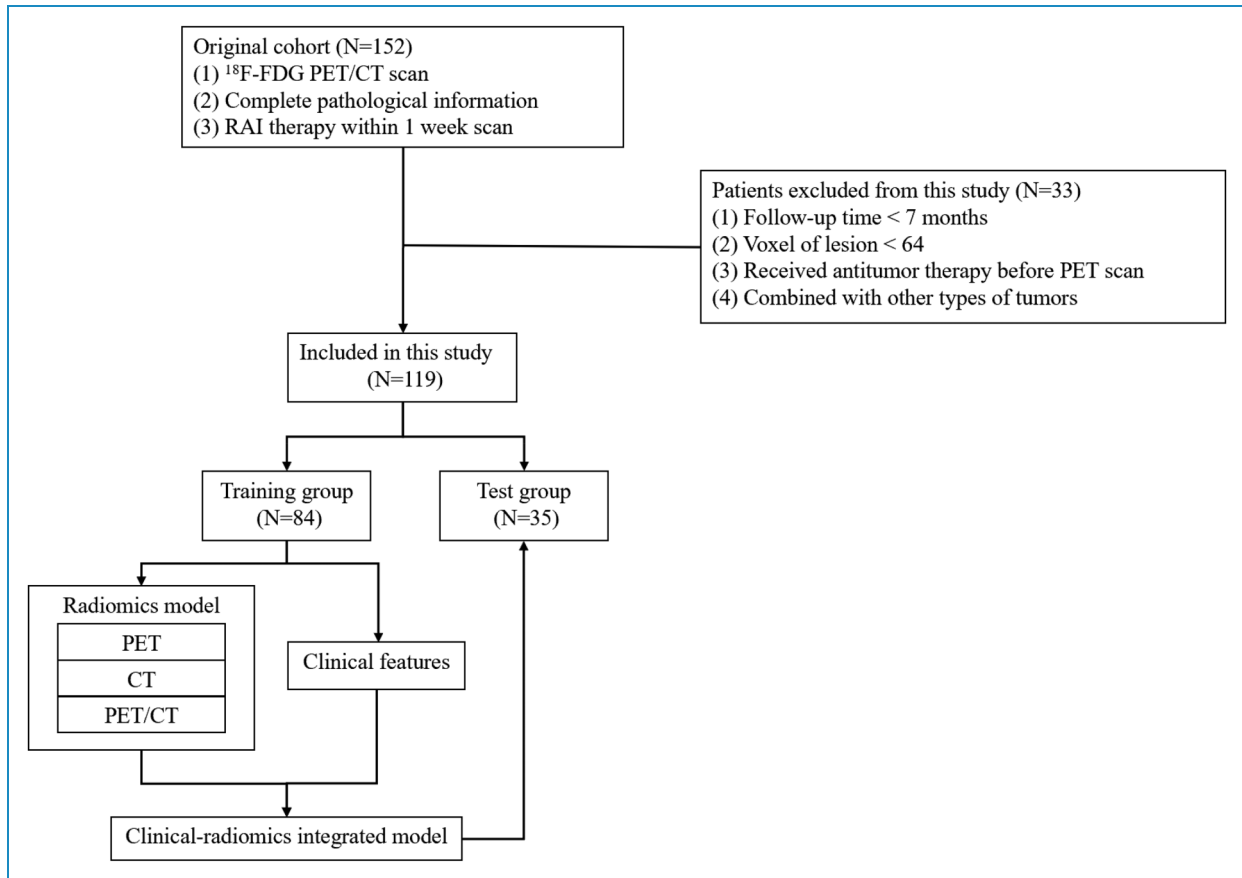


Figure 1. Flow chart of study design.

Texture feature extraction and analysis of multimodal images

CT and PET images were imported into LIFEx software, with regions of interest (ROI) delineated and texture features extracted based on LIFEx version 7.3.0.¹⁴ A nuclear medicine physician with five years of diagnostic experience in head and neck imaging delineated the ROI layer by layer for the abnormal lymph node lesions to be analyzed, aiming to maintain consistency with the lesion edge. In cases of uncertainty, coronal and sagittal images were used to obtain a three-dimensional volume of interest (VOI). Principles of ROI delineation included the following: delineating typical lymph node lesions that met the diagnostic requirements of CT and PET/CT; discarding lesions with blurred margins and unclear borders of surrounding soft tissues and outlining along the edge of the lesion while enlarging it appropriately to include all lesions within the ROI. To delineate the region of interest, the location of the lesion on the PET/CT fusion image was determined. The ROI was outlined on the CT image after hiding the PET image, and the same ROI was applied to the PET image to extract PET and CT features separately.

Clinical information collection and follow-up

Clinical information collected included patients' TSH (values >150 mIU/L were considered as 150), Tg and TgAb (values <10 were considered as 10 IU/ml and values >1000 were considered as 1000 IU/ml). TNM staging was conducted based on patients' histopathological results after surgery.¹⁵ The median follow-up time for patients was 28 months, with an average follow-up time of 27.5 ± 14.8 months.

Scanners and capture protocol

PET/CT images in this study were acquired using a uMI 510 PET/CT scanner from United Imaging. ¹⁸F-FDG was produced and provided by Shanghai Xinke Pharmaceutical Co., Ltd, with a radiochemical purity of >95%. Before examination, patients fasted for over 6 h, maintained blood glucose levels <11.0 mmol/L and received an intravenous injection of 3.7–5.55 MBq/Kg ¹⁸F-FDG based on their weight. Patients rested quietly for 60 min after the injection.

During scanning, patients were positioned supine and the scanning range extended from the base of the skull to the upper 1/3 of the femur. After selecting the examination

range, helical CT scanning was performed with a tube voltage of 120 kV, tube current of 60–100 mAs and slice thickness of 5.0 mm. PET image reconstruction utilized the ordered subset expectation maximization (OS-EM), with image attenuation correction performed using CT scan data. Standard reconstruction methods were employed for CT reconstruction, and the reconstruction slice thickness was set at 5 mm.

Multimodal model construction and effectiveness evaluation

We set the number of seeds to 300 and divided the original cohort into a training group and a test group at a 7:3 ratio. The least absolute shrinkage and selection operator (LASSO) was used to further screen the different features, and the selected texture features were used to construct the model in training group. LASSO regression was used to screen features among CT, PET and PET/CT features, respectively. CT, PET and PET/CT models were established separately, and their diagnostic performances were analyzed using ROC curves. The optimal radiomics model was combined with clinical features to establish a nomogram model, and then the stability and effectiveness of the model in the validation group were analyzed through calibration curve, ROC curve and C-index.

Image analysis

For lymph node lesions with increased FDG uptake, the final diagnosis was made by two nuclear medicine physicians with over 10 years of experience in PET/CT diagnosis, who examined positive uptake lesions in combination with CT images while concealing the patients' medical history and other clinical data. The criterion for characterizing lymph node lesions was based on clinical follow-up.

Statistical analysis

SPSS 26.0, R 4.2.2 and MedCalc statistical software were used for analysis. Continuous variables were described as mean \pm standard deviation. Texture analysis data were subjected to the Mann–Whitney U test, and $p < 0.05$ was considered statistically significant. Logistic regression was used to calculate the radiomics score, and the difference in diagnostic efficacy was analyzed using the DeLong test.

Results

Baseline information

Among the study participants, 54 patients were confirmed to have lymph node metastasis of thyroid cancer, while 65 patients belonged to the non-metastasis

group. A total of 119 lymph node lesions were delineated. The baseline information for the patients is presented in Table 1.

Table 1. Baseline information of included patient in training and test group.

	Training group (n = 84)	Test group (n = 35)
Age (years)	42.81 \pm 13.08	44.34 \pm 14.07
Sex (M/F)	30/54	16/19
BMI	24.79 \pm 3.52	24.83 \pm 4.27
TNM stage		
I	69	26
II	1	2
III	9	1
IV	5	6
Lymph node location		
I	15	5
II	36	16
III	6	4
IV	11	5
V	4	1
VI	0	0
VII	7	3
Supraclavicular	5	1
SUVmax	8.28 \pm 10.68	12.90 \pm 19.19
Length	12.40 \pm 4.27	13.23 \pm 5.23
Width	6.92 \pm 2.31	7.56 \pm 3.00
L/W	1.85 \pm 0.56	1.79 \pm 0.33
TSH	102.80 \pm 37.71	106.59 \pm 37.98
Tg	79.79 \pm 199.55	154.43 \pm 595.24
TgAb	107.89 \pm 242.22	145.03 \pm 317.55
Tg/TgAb	7.27 \pm 19.52	15.29 \pm 59.56

Table 2. Lymph node distribution and clinical features of patients in training group.

	Metastasis (n = 37)	Non-metastasis (n = 47)	P
Age (years)	67.24 ± 28.12	41.06 ± 11.99	0.169
Sex (M/F)	16/21	14/33	0.201
BMI	24.48 ± 3.33	25.04 ± 3.69	0.474
TNM stage			0.593
I	29	40	
II	1	0	
III	4	5	
IV	3	2	
SUVmax	11.79 ± 14.94	5.52 ± 3.65	0.007
Length	13.36 ± 4.20	11.65 ± 4.22	0.067
Width	7.28 ± 2.16	6.63 ± 2.41	0.197
L/W	1.89 ± 0.51	1.82 ± 0.61	0.628
TSH	96.19 ± 39.35	108.00 ± 35.94	0.156
Tg	162.28 ± 280.09	14.86 ± 25.90	0.001
TgAb	86.81 ± 212.49	124.50 ± 264.36	0.482
Tg/TgAb	14.74 ± 27.69	1.40 ± 2.60	0.001

Differences between lymph node metastases and non-metastatic lesions in the training group

The location distribution, imaging features and serological examination results of the lymph node lesions were analyzed (Table 2). The results showed that there were statistically significant differences in SUVmax and Tg between the metastatic and non-metastatic groups.

Development and comparison of multimodal radiomics models

For each lesion, 164 CT texture features and 164 PET texture features were extracted, with 107 parameters of varying significance identified, including 16 CT texture parameters and 91 PET texture parameters. LASSO regression was used to screen radiomics parameters for CT, PET and PET/CT models. Ultimately, 3 CT parameters, 4 PET

parameters and 12 PET/CT parameters were selected to establish three models (Figure 2). The diagnostic performance of the three models was analyzed using ROC curves, resulting in AUC (CT)=0.730, AUC (PET)=0.759 and AUC (PET/CT)=0.864. The difference between PET/CT and CT was statistically significant ($p=0.0047$) (Figure 3). Subsequently, the radscore value and formula for each patient were derived based on the results of the PET/CT model established by binary logistic regression analysis (Supplemental Material 1).

Diagnostic efficacy of radiomics score combined with clinical features

We performed univariate and multivariate analyses on the radscore obtained from the previously established PET/CT model and the clinical features of the patients in the training group with lymph node metastasis. In order to ensure the robustness of the radiomics results, we conducted a secondary delineation of the data in the training group and performed intraclass correlation coefficient (ICC) analysis on the modeling features. The results showed that most of the radiomics features used for modeling had relatively good consistency (Supplemental Table 1). We included clinical features such as age, gender, tumor TNM stage and an important biochemical indicator in thyroid cancer. The results of the univariate analysis showed that age and stage were risk factors; however, there was no significant statistical difference. Considering the clinical significance, we still included these clinical features in the multivariate analysis (Table 3).

Nomogram construction and evaluation

We constructed a nomogram that combined radiomics with clinical features to evaluate the risk of metastasis after thyroid surgery (Figure 4A). The calibration curve for the metastasis risk nomogram was used to predict the metastasis risk before RAI therapy, the Brier score=0.11 (Figure 4B). The C-index and AUC for the prediction nomogram was 0.915 in the training group. In the training group, the diagnostic efficacy of the model established by clinical features was AUC=0.818, and the difference in diagnostic efficacy of the model established by combining radscore was statistically significant through the DeLong test (0.915 vs. 0.818, $P=0.0126$). In the testing group, the C-index was confirmed to be 0.868. The results of the calibration curve, ROC curve and C-index indicate the nomogram model's good discrimination. The decision curve showed that if the threshold probability for a patient and a doctor is >4%, using this nomogram to predict metastasis risk adds more benefit than the alternative scheme (Figure 4C).

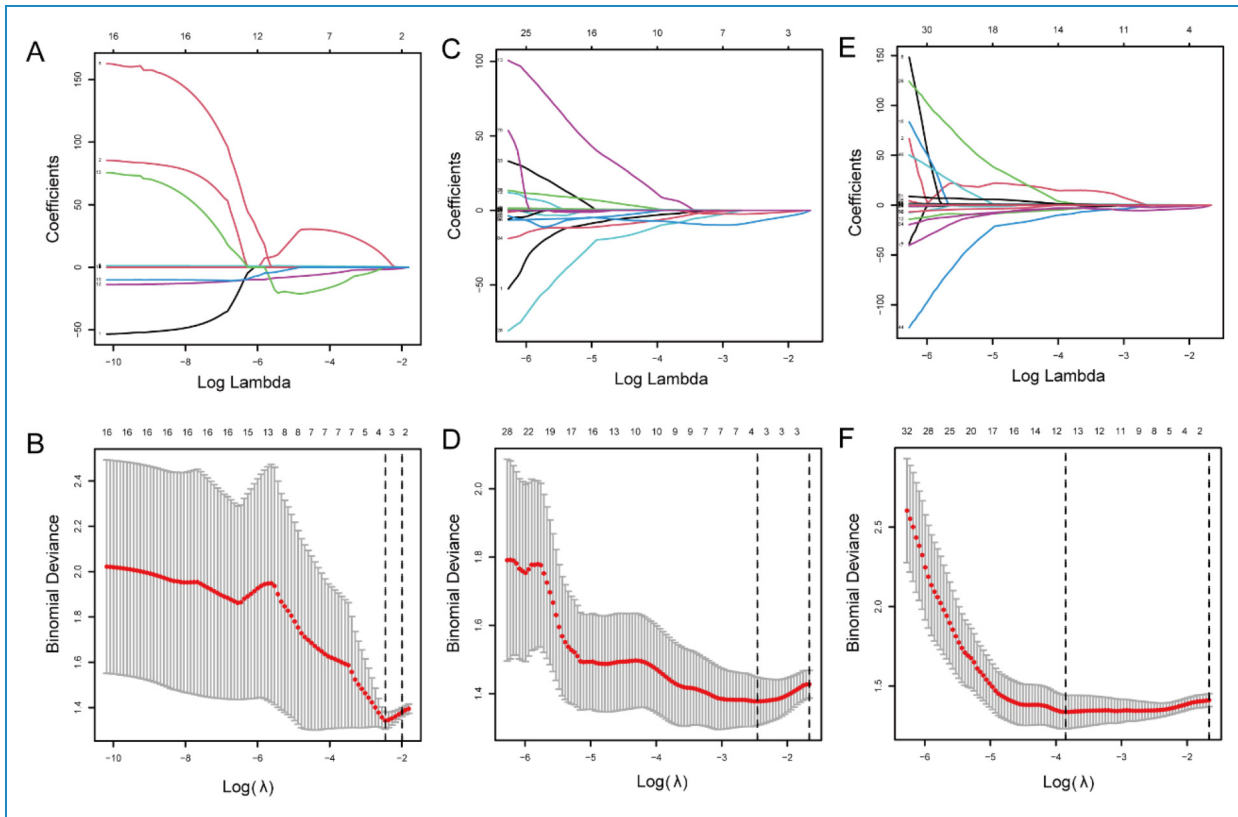


Figure 2. LASSO regression screening parameters of multimodal radiomics model and evaluation of diagnostic efficacy after modeling. (A, B) Screening of CT radiomics parameters. (C, D) Screening of PET radiomics parameters. (E, F) Screening of PET/CT radiomics parameters.

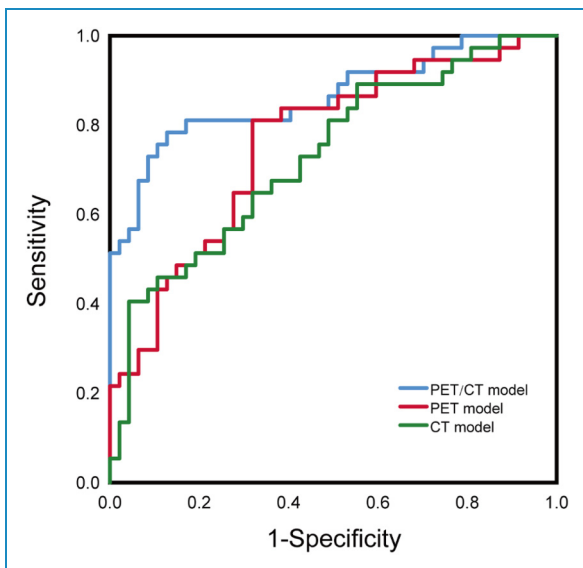


Figure 3. CT, PET and PET/CT model ROC curve analysis in the training group.

Discussion

Lymph node metastasis after thyroid cancer surgery has consistently posed challenges for both clinicians and

patients. Thyroid cancer is a prevalent malignant tumor, with surgical resection being one of its primary treatments. Postoperative lymph node metastasis is a crucial factor influencing the prognosis of thyroid cancer. Our study enhances the diagnostic performance of lymph node metastases after thyroid surgery by employing a multimodal texture analysis method. Conducting a comprehensive assessment before radioactive iodine treatment allows for a more accurate and systematic evaluation of the patient's condition, which includes postoperative thyroid remnants, lymph node metastasis and distant metastasis. This provides valuable insights for devising treatment plans for radioactive iodine therapy, thereby improving prognosis and minimizing unnecessary radiotherapy.

To our knowledge, this is the first study to apply texture analysis to the investigation of lymph node metastases after thyroid cancer surgery and to incorporate multimodal data and clinical features. While most researchers have focused on the impact of the primary tumor and patient survival, the effects of metastases on patients' quality of life and prognosis have often been overlooked. Through the feature selection and multimodal radiomics model construction presented in this study, it is evident that the metabolic information derived from PET offers a better distinction of lymph node metastasis compared to purely anatomical

Table 3. Univariate and multivariate analysis of radiomics and clinical features.

	No. of patients	Univariate analysis		Multivariate analysis	
		HR and 95% CI	P	HR and 95% CI	P
Age					
<55	62				
≥55	22	2.287 (0.848, 6.165)	0.102	0.803 (0.075, 8.658)	0.857
Gender					
Male	30				
Female	54	0.557 (0.226, 1.372)	0.203	1.025 (0.240, 4.381)	0.973
Stage					
I	69				
II-IV	15	1.576 (0.514, 4.838)	0.426	1.896(0.103, 35.029)	0.667
Tg					
<20	44				
≥20	40	11.864 (4.220, 33.355)	<0.001	6.410 (1.518, 27.066)	0.011
Radscore					
<0.4	50				
0.4-0.6	5	7.875 (1.129, 54.931)	0.037	14.213 (1.405, 143.744)	0.025
≥0.6	29	45.500 (11.062, 187.145)	<0.001	22.764 (4.395, 117.906)	<0.001

information. Previous research has demonstrated that in the ablation of thyroid remnants, FDG PET results can predict long-term survival, further highlighting that tissue metabolic characteristics may encompass more abundant information than anatomical features alone from CT.¹⁶ The selection of texture analysis methods is crucial, and previous research has confirmed the robustness and feasibility of LIFEx for extracting texture features.¹⁷⁻²² The radscore we developed integrates both PET and CT data, and the nomogram model, combined with clinical features, demonstrates a high degree of discrimination. The stability and accuracy of the results are further validated by the test set. A previous study that differentiated metastases from primary tumors also showed that PET radiomics signatures possess superior discriminative power and exhibit potential for identifying disease subtypes.²³ The meanings of the features used to establish the model are described in detail in Supplemental Table 3. Most of the features used to establish the model are used to present the characteristics of image

uniformity, size and pixel intensity distribution. In addition, the modeling CT features include texture feature describing calcification, which may be related to the presence of calcification in some metastatic lymph nodes, which is also a characteristic of PTC.

Diagnosing postoperative lymph node metastasis necessitates a combination of multiple imaging examinations, such as ultrasound, CT and MRI. These examinations assist doctors in determining the location, size and number of lymph node metastases. Histopathological results following lymph node resection remain the gold standard for diagnosing postoperative lymph node metastasis. However, each diagnostic method has its limitations. Invasive histopathological examination may also compromise diagnostic efficiency due to sampling errors. Thus, enhancing the accuracy of non-invasive diagnosis is a feasible strategy. We established a radiomics score and incorporated available clinical feature information, which offers better translational feasibility compared to artificial intelligence approaches. We established

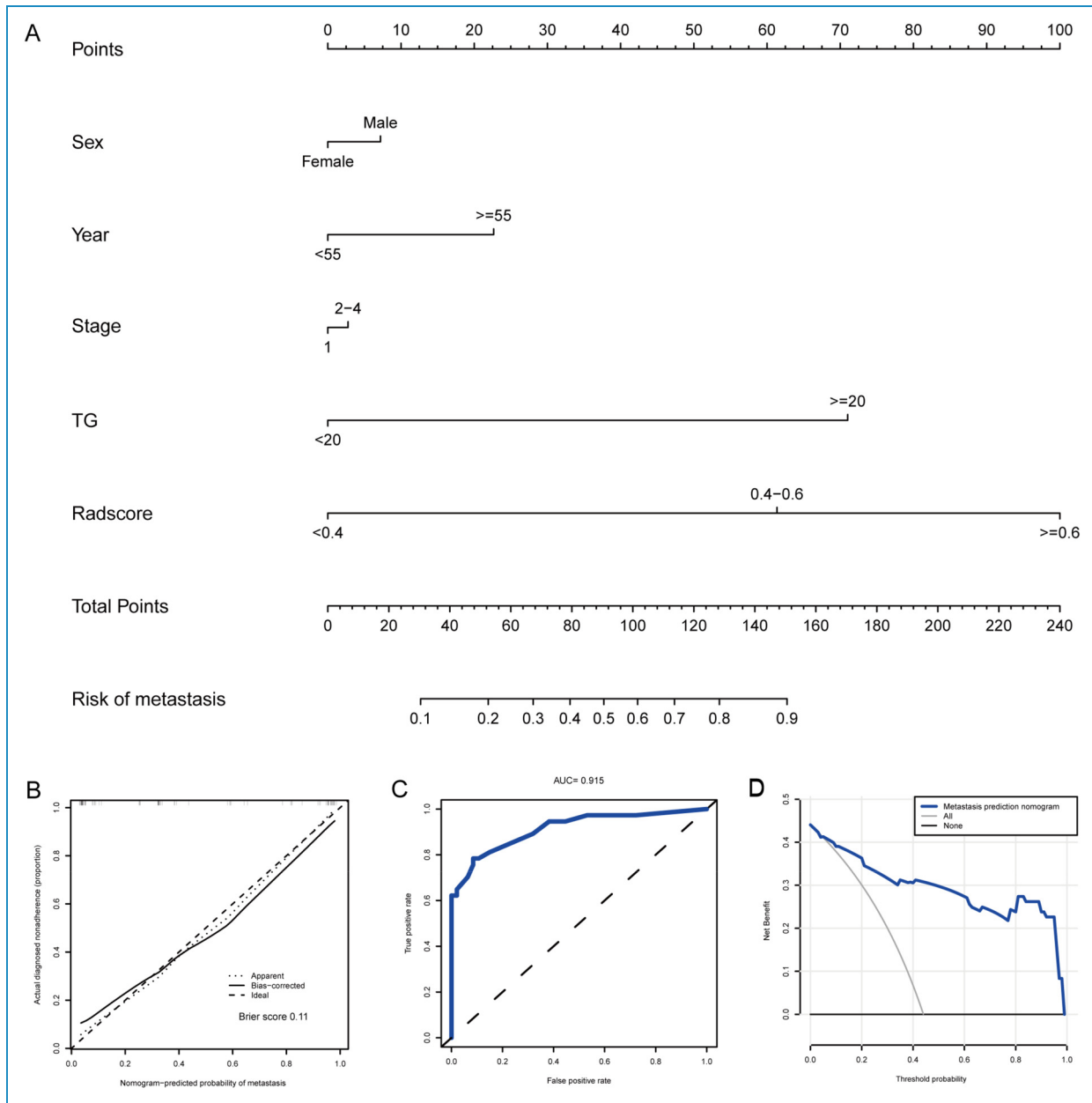


Figure 4. The nomogram construction and evaluation. (A) The nomogram of radiomics and clinical features. (B) Calibration curves of the metastasis nomogram prediction in the training group. (C) ROC curve of the nomogram prediction in the training group. (D) Decision curve analysis for the metastasis nomogram.

a multimodal radiomics model that combined the CT and PET radiomics features and significantly improved the diagnostic performance compared with a separate clinical feature model. However, the model still exhibits instances of false positives and false negatives, as illustrated in Supplemental Figures 1 and 2. Patients exhibiting a low SUVmax and possessing only one risk factor, such as elevated Tg levels, are more susceptible to false-positive diagnoses. Conversely, lesions that do not show a significant increase in SUVmax uptake are at a higher risk of yielding false-negative results. Previous studies

have found that in breast and lymph node lesions, expanding the delineated area of lesions to include part of the tumor microenvironment may improve the diagnostic performance of the disease.²⁴ Whether this will have the same effect in metastatic lymph nodes of thyroid cancer deserves further exploration in the future. Radiomics has conducted a series of studies in the field of diagnosis related to thyroid cancer. In addition to combining with pathology and follow-up results to determine the benign and malignant disease and prognosis, nuclear medicine imaging can also be combined with ultrasound imaging to determine

nodules' iodine uptake. Whether it is a "cold nodule" or a "hot nodule" is also a meaningful research direction.²⁵

Accurate diagnosis of postoperative lymph node metastasis in thyroid cancer is vital for prognosis. To improve thyroid cancer prognosis, some researchers have conducted ¹²⁴I-NaI PET/CT imaging in the early stage. While this is a feasible method, it has limitations for thyroid cancer with poorly differentiated and radioiodine refractory characteristics.²⁶ The combination of different target imaging agents may improve the diagnostic efficiency of thyroid cancer metastases. Fibroblast activation protein (FAP) is an emerging target in the field of nuclear medicine diagnosis. Studies have shown that fibroblast activation protein inhibitor (FAPI) has higher detection sensitivity for thyroid cancer metastases than FDG.^{27–29} For recurrent PTC, especially when Tg levels are high, ⁶⁸Ga-FAPI can be used in patients with inconclusive ¹⁸F-FDG results.³⁰ In addition to FAPI, studies have shown that the expression of prostate-specific membrane antigen (PSMA) is related to the degree of differentiation of thyroid cancer and may indicate the persistence and recurrence of thyroid cancer.^{31,32} Numerous guidelines exist for thyroid cancer, and reference standards are inconsistent. Our study provides a reference for imaging, especially for individuals with an intermediate risk of recurrence, where PET/CT examination is highly significant.^{33,34} With the current high recurrence rate of thyroid cancer, our research results may help reduce recurrence and improve post-surgery prognosis.³⁵ In later stages, monitoring the survival of patients with distant metastases after treatment can further refine patient management guidelines.³⁶

Our study has some limitations. Firstly, being a single-center study, the possibility of residual confounding factors, both known and unknown, cannot be dismissed. Secondly, our delineation criteria, requiring a minimum of 64 voxels, might lead to the exclusion of smaller lesions that are visible. The impact of small lymph node metastasis on disease progression is subject to mixed findings in the literature: some studies suggest an increased risk of disease recurrence,³⁷ while others report no significant effect on prognosis.³⁸ This variability emphasizes the need for advanced radiomics technology capable of automated and precise identification of small lesions. Additionally, our exclusion of cases where lymph node margins were indiscernible could introduce bias. Finally, the retrospective design of our study is accompanied by inherent limitations typical of such research approaches. These limitations emphasize the necessity for future research endeavors. Prospective, large-scale, multi-center studies are essential for a more precise assessment of radiomics' effectiveness in the diagnosis of lymph node metastases in thyroid cancer.

Conclusion

Radiomics has the potential to enhance the diagnostic efficiency of lymph node metastases after thyroid cancer

surgery and may be utilized to assist doctors in clinical diagnosis in the future. By combining radiomics with clinical features, we developed a novel nomogram that demonstrates relatively good accuracy, helping clinicians assess the risk of metastasis in thyroid patients after surgery.

Acknowledgment: The authors thank the LIFEx development team for their software support.

Contributorship: All authors contributed to the study conception and design. XF, HZ, ZW and XZ contributed to data collection and analysis. JZ and FY contributed to language editing and polishing. XF, SQ, JZ, FH and MY contributed to patient follow-up. The first draft of the manuscript was written by XF, FY and all authors commented on previous versions of the manuscript. All authors read and approved the final manuscript.


Declaration of conflicting interests: The authors declared no potential conflicts of interest with respect to the research, authorship, and/or publication of this article.

Ethics Approval: This study was performed in line with the principles of the Declaration of Helsinki. Approval was granted by the Ethics Committee of Shanghai Tenth People's Hospital (SHYS-IEC-5.0/22K263/P01).

Funding: The authors disclosed receipt of the following financial support for the research, authorship, and/or publication of this article: This work was conducted with the support by the explorer program of the Science and Technology Commission of Shanghai Municipality (22TS1400500).

Guarantor: FY

Informed Consent: As this was a retrospective study, a waiver of informed consent was requested from the ethics committee and approved.

ORCID iD: Fei Yu  <https://orcid.org/0000-0003-2951-725X>

Data availability statement: The datasets generated during and/or analyzed during the current study are available from the corresponding authors on reasonable request.

Supplemental material: Supplemental material for this article is available online.

References

1. Cooper DS, Doherty GM, Haugen BR, et al. Revised American Thyroid Association management guidelines for patients with thyroid nodules and differentiated thyroid cancer. *Thyroid* 2009; 19: 1167–1214.

2. Siddiqui S, White MG, Antic T, et al. Clinical and pathologic predictors of lymph node metastasis and recurrence in papillary thyroid microcarcinoma. *Thyroid* 2016; 26: 807–815.
3. Juweid ME, Tulchinsky M, Mismar A, et al. Contemporary considerations in adjuvant radioiodine treatment of adults with differentiated thyroid cancer. *Int J Cancer* 2020; 147: 2345–2354.
4. Albano D, Bonacina M, Durmo R, et al. Efficacy of low radioiodine activity versus intermediate-high activity in the ablation of low-risk differentiated thyroid cancer. *Endocrine* 2020; 68: 124–131.
5. Molenaar RJ, Sidana S, Radivoyevitch T, et al. Risk of hematologic malignancies after radioiodine treatment of well-differentiated thyroid cancer. *J Clin Oncol* 2018; 36: 1831–1839.
6. Piscopo L, Volpe F, Nappi C, et al. Second primary malignancies in patients with differentiated thyroid cancer after radio-nuclide therapy: a retrospective single-centre study. *Curr Oncol* 2022; 30: 37–44.
7. Zampella E, Klain M, Pace L, et al. PET/CT in the management of differentiated thyroid cancer. *Diagn Interv Imaging* 2021; 102: 515–523.
8. Haugen BR, Alexander EK, Bible KC, et al. American thyroid association management guidelines for adult patients with thyroid nodules and differentiated thyroid cancer: the American thyroid association guidelines task force on thyroid nodules and differentiated thyroid cancer. *Thyroid* 2015; 2016: 1–133.
9. Pan L, Chen Y, Li S, et al. Postoperative thyroid remnants for differentiated thyroid cancer may not affect the outcome of high-dose radioiodine therapy. *Oral Oncol* 2020; 104: 104610.
10. Tsang JF, Levin DP and Leslie WD. Thyroglobulin flare response after radioiodine ablation in 2 patients with differentiated thyroid cancer. *Clin Nucl Med* 2015; 40: 421–422.
11. Guo P, Wang X, Xia L, et al. Analysis of factors associated with the prognosis of papillary thyroid cancer and the construction of a survival model. *Cancer Med* 2023; 12: 7868–7876.
12. Liu W, Zhang D, Jiang H, et al. Prediction model of cervical lymph node metastasis based on clinicopathological characteristics of papillary thyroid carcinoma: a dual-center retrospective study. *Front Endocrinol (Lausanne)* 2023; 14: 1233929.
13. Zheng H, Lai V, Lu J, et al. Clinical factors predictive of lymph node metastasis in thyroid cancer patients: a multivariate analysis. *J Am Coll Surg* 2022; 234: 691–700.
14. Nioche C, Orhac F, Boughdad S, et al. LIFEx: a freeware for radiomic feature calculation in multimodality imaging to accelerate advances in the characterization of tumor heterogeneity. *Cancer Res* 2018; 78: 4786–4789.
15. Amin MB, Greene FL, Edge SB, et al. The eighth edition AJCC cancer staging manual: continuing to build a bridge from a population-based to a more “personalized” approach to cancer staging. *CA Cancer J Clin* 2017; 67: 93–99.
16. Gaertner FC, Okamoto S, Shiga T, et al. FDG PET performed at thyroid remnant ablation has a higher predictive value for long-term survival of high-risk patients with well-differentiated thyroid cancer than radioiodine uptake. *Clin Nucl Med* 2015; 40: 378–383.
17. Antunovic L, De Sanctis R, Cozzi L, et al. PET/CT radiomics in breast cancer: promising tool for prediction of pathological response to neoadjuvant chemotherapy. *Eur J Nucl Med Mol Imaging* 2019; 46: 1468–1477.
18. Fiz F, Masci C, Costa G, et al. PET/CT-based radiomics of mass-forming intrahepatic cholangiocarcinoma improves prediction of pathology data and survival. *Eur J Nucl Med Mol Imaging* 2022; 49: 3387–3400.
19. Kirienco M, Cozzi L, Antunovic L, et al. Prediction of disease-free survival by the PET/CT radiomic signature in non-small cell lung cancer patients undergoing surgery. *Eur J Nucl Med Mol Imaging* 2018; 45: 207–217.
20. Li Y, Zhang Y, Fang Q, et al. Radiomics analysis of [(18)F]FDG PET/CT for microvascular invasion and prognosis prediction in very-early- and early-stage hepatocellular carcinoma. *Eur J Nucl Med Mol Imaging* 2021; 48: 2599–2614.
21. Zhou Y, Ma XL, Zhang T, et al. Use of radiomics based on (18)F-FDG PET/CT and machine learning methods to aid clinical decision-making in the classification of solitary pulmonary lesions: an innovative approach. *Eur J Nucl Med Mol Imaging* 2021; 48: 2904–2913.
22. Larobina M, Megna R and Solla R. Comparison of three freeware software packages for (18)F-FDG PET texture feature calculation. *Jpn J Radiol* 2021; 39: 710–719.
23. Kirienco M, Cozzi L, Rossi A, et al. Ability of FDG PET and CT radiomics features to differentiate between primary and metastatic lung lesions. *Eur J Nucl Med Mol Imaging* 2018; 45: 1649–1660.
24. Mohammadi A, Mirza-Aghazadeh-Attari M, Faeghi F, et al. Tumor microenvironment, radiology, and artificial intelligence: should we consider tumor periphery? *J Ultrasound Med* 2022; 41: 3079–3090.
25. Ardakani AA, Mohammadzadeh A, Yaghoubi N, et al. Predictive quantitative sonographic features on classification of hot and cold thyroid nodules. *Eur J Radiol* 2018; 101: 170–177.
26. Sabet A, Binse I, Grafe H, et al. Prognostic impact of incomplete surgical clearance of radioiodine sensitive local lymph node metastases diagnosed by post-operative (124)I-NaI-PET/CT in patients with papillary thyroid cancer. *Eur J Nucl Med Mol Imaging* 2016; 43: 1988–1994.
27. Fu H, Fu J, Huang J, et al. 68Ga-FAPI PET/CT versus 18F-FDG PET/CT for detecting metastatic lesions in a case of radioiodine-refractory differentiated thyroid cancer. *Clin Nucl Med* 2021; 46: 940–942.
28. Fu H, Fu J, Huang J, et al. 68Ga-FAPI PET/CT in thyroid cancer with thyroglobulin elevation and negative iodine scintigraphy. *Clin Nucl Med* 2021; 46: 427–430.
29. Fu H, Wu J, Huang J, et al. (68)Ga fibroblast activation protein inhibitor PET/CT in the detection of metastatic thyroid cancer: comparison with (18)F-FDG PET/CT. *Radiology* 2022; 304: 397–405.
30. Sayiner ZA, Elboğa U, Sahin E, et al. Comparison of (68)Ga-FAPI-04 and (18)F-FDG PET/CT for diagnosis of metastatic lesions in patients with recurrent papillary thyroid carcinoma. *Hell J Nucl Med* 2023; 26: 41–46.
31. Ciappuccini R, Saguet-Rysanek V, Giffard F, et al. PSMA Expression in differentiated thyroid cancer: association with radioiodine, 18FDG uptake, and patient outcome. *J Clin Endocrinol Metab* 2021; 106: 3536–3545.

32. Feng YY, Shi YR, Xia Z, et al. The clinical signification and application value of [(68)Ga]Ga-PSMA imaging in thyroid malignancy. *Endocrine* 2023. DOI:10.1007/s12020-023-03599-x.
 33. Schlumberger M and Leboulleux S. Current practice in patients with differentiated thyroid cancer. *Nat Rev Endocrinol* 2021; 17: 176–188.
 34. Pacini F, Fuhrer D, Elisei R, et al. ETA consensus statement: what are the indications for post-surgical radioiodine therapy in differentiated thyroid cancer? *Eur Thyroid J* 2022; 2022: 11.
 35. Nunes KS, Matos LL, Cavalheiro BG, et al. Risk factors associated with disease-specific mortality in papillary thyroid cancer patients with distant metastases. *Endocrine* 2022; 75: 814–822.
 36. Albano D, Bertagna F, Bonacina M, et al. Possible delayed diagnosis and treatment of metastatic differentiated thyroid cancer by adopting the 2015 ATA guidelines. *Eur J Endocrinol* 2018; 179: 143–151.
 37. Rowe ME, Ozbek U, Machado RA, et al. The prevalence of extranodal extension in papillary thyroid cancer based on the size of the metastatic node: adverse histologic features are not limited to larger lymph nodes. *Endocr Pathol* 2018; 29: 80–85.
 38. Randolph GW, Duh QY, Heller KS, et al. The prognostic significance of nodal metastases from papillary thyroid carcinoma can be stratified based on the size and number of metastatic lymph nodes, as well as the presence of extranodal extension. *Thyroid* 2012; 22: 1144–1152.
-